MIJST
MIST International Journal of Science and Technology

Potential Health Impacts from Radioactive Releases at Rooppur Nuclear Power Plant Under Hypothetical Accident Scenario

Md Rosaidul Mawla[1,*], Radmim Ryean[1], Anisur Rahman[2], Abdus Sattar Mollah[3], Md. Shafiqul Islam[4], Kazi Imtiaz Kabir[5]

[1]Department of Electrical, Electronic and Communication Engineering, Military Institute of Science and Technology, Mirpur 1216, Dhaka, Bangladesh
[2]Center for Research Reactor, Atomic Energy Research Establishment, Savar 1349, Bangladesh
[3]Department of Nuclear Science and Engineering, Military Institute of Science and Technology, Mirpur 1216, Dhaka, Bangladesh
[4]Department of Nuclear Engineering, University of Dhaka, Dhaka 1000, Bangladesh
[5]Research and Development Wing, Military Institute of Science and Technology, Mirpur 1216, Dhaka, Bangladesh

***Corresponding Email:** *mawla71@yahoo.com*

ARTICLE INFO

Article History:

Received: 04th July 2025
Revised: 08th May 2025
Accepted: 12th May 2025
Published: 30th December 2025

Keywords:

Total Effective Dose
Committed Effective Dose
Thyroid Dose
Radiological Health Risk
Nuclear Accident

ABSTRACT

This study presents a comprehensive assessment of radiological dose consequences from potential severe accident scenarios at the Rooppur Nuclear Power Plant (NPP), focusing on health impacts from radioactive releases. Utilizing HotSpot 3.1.2 and ORIGEN 2.2, the research estimates Total Effective Dose Equivalent (TEDE) and Committed Effective Dose Equivalent (CEDE) to critical organs, including the thyroid, skin, lungs, surface bone, red marrow, and liver, under seasonal meteorological conditions. The thyroid, due to its high affinity for radioactive iodine (particularly 131I), showed maximum CEDE values of 8.0 × 105 Sv and 4.4 × 105 Sv during the autumn and rainy seasons, respectively, at 30 meters from the source. These values, along with other organ doses, exceeded public and occupational dose limits up to 15 km in the rainy season and 30 km in the autumn season, primarily influenced by wind speed and precipitation. The study underscores the need for emergency protective measures such as sheltering, evacuation, and the administration of potassium iodide (KI), especially for populations within high-risk zones. It further recommends the integration of dose modeling findings into the National Nuclear and Radiological Emergency Preparedness and Response Plan (NNREPRP) to enhance response strategies and protect public health in the event of nuclear accidents.

1. INTRODUCTION

Nuclear energy plays a pivotal role in supporting the sustainable development goals by delivering low-carbon, high-capacity power that enhances both energy security and environmental sustainability. Achieving sustainable development necessitates a reliable and affordable energy infrastructure capable of minimizing greenhouse gas emissions, supporting healthcare and education systems, fostering industrialization, and reducing poverty. Nuclear power, when integrated with other advanced energy technologies, can meet these demands while promoting long-term economic resilience and environmental protection (Rogner, 2001; Sattar et al., 2016). In alignment with these goals, Bangladesh is commissioning the Rooppur Nuclear Power Plant (NPP), comprising two VVER-1200 units designed under the Generation III+ ASE-2006 specifications. These reactors are expected to become operational by 2025/2026 and are equipped with enhanced passive and active safety systems, offering increased resistance to severe accidents (Fairuz and Sahadath, 2020). Nevertheless, the possibility of a low-probability, high-consequence event cannot be entirely dismissed and warrants thorough risk assessment and emergency preparedness planning.

The International Atomic Energy Agency (IAEA) defines a nuclear accident as an event involving the release of radioactive materials that has significant consequences for the environment, the public, and the nuclear facility where it occurs (IAEA, 2013). When safety systems fail to operate as designed, such events can escalate into severe accidents with profound impacts on human health (Aliyu et al., 2015) and the surrounding environment. During a

nuclear accident, radionuclides such as iodine-131 (^{131}I), cesium-137 (^{137}Cs), and strontium-90 (^{90}Sr) may be released, emitting gamma rays, beta particles, and alpha particles. These forms of radiation vary in their penetration capabilities and biological effects. The severity of health outcomes depends on the type and amount of radiation, duration of exposure, and individual susceptibility. Short-term effects may include acute radiation syndrome, nausea, burns, and immune suppression, while long-term effects can involve cancer, organ damage, reproductive issues, and hereditary mutations.

Historical nuclear accidents provide critical insight into the nature and consequences of radioactive releases. The Chernobyl disaster in 1986 resulted in the release of a wide range of radionuclides, with iodine-131 (^{131}I) and cesium-137 (^{137}Cs) having the most significant impact on public health and the environment due to their radiological properties and biological uptake (Sihver and Yasuda, 2018). Similarly, the Fukushima Daiichi accident in 2011 led to the release of several volatile fission products, including noble gases like krypton-85 (^{85}Kr) and xenon-133 (^{133}Xe), as well as isotopes of iodine (^{131}I, ^{132}I), cesium (^{134}Cs, ^{136}Cs, ^{137}Cs), and tellurium (^{132}Te) (Faith and Kim, 2020). Studies on previous nuclear power plant accidents confirm that these radionuclides, particularly noble gases (xenon and krypton), iodine, cesium, strontium, tellurium, and rubidium are among the most likely to be released during a severe event (ICRU, 2015; Faith and Kim, 2020). These substances vary in terms of their physical and chemical properties, environmental mobility, and biological effects, making them critical indicators for dose assessment and emergency planning. These past incidents highlight the necessity of understanding the behavior and health implications of specific radionuclides in order to enhance preparedness and response strategies for nuclear facilities, including the Rooppur NPP in Bangladesh.

Radioactive releases during nuclear accidents pose serious health risks, with iodine-131 (^{131}I) and cesium-137 (^{137}Cs) being the most critical radionuclides. ^{131}I has a short half-life of about eight days and accumulates in the thyroid gland when inhaled or ingested, increasing the risk of thyroid cancer (Walsh et al., 2014, Faith and Kim, 2020), particularly in children. In contrast, ^{137}Cs, with a 30-year half-life, contaminates soil and food supplies, leading to long-term exposure and impacts on agriculture (Yasunari et al., 2011), livestock, and human health (Hoeve and Jacobson, 2012; Aliyu et al., 2015).

Assessing radiation dose is essential for understanding these risks. Dose assessment considers external, inhalation, and ingestion pathways to estimate the Total Effective Dose Equivalent (TEDE) and Committed Effective Dose Equivalent (CEDE). The thyroid gland receives special attention due to its sensitivity to radioiodine. Based on dose assessments, protective measures such as sheltering, evacuation, food restrictions, and potassium iodide distribution are used to minimize health effects.

This research focuses on a hypothetical major radioactive release at the Rooppur NPP, which houses Generation III+ VVER-1200 reactors. While limited studies exist globally on VVER-1200 accident scenarios, few integrate detailed source term modeling, meteorological analysis, and radiation dispersion together. This study bridges that gap by combining source term estimation using ORIGEN 2.2 (Croff, 1980; Croff, 1983), wind pattern simulation via wind rose analysis, and atmospheric dispersion and dose modeling with HotSpot Health Physics software (Homann and Aluzzi, 2013).

This study aims to estimate potential radiation doses to **human organs** and the **environment** under a severe accident scenario at Rooppur NPP using a **site-specific** and **seasonally** differentiated approach. By integrating reactor source term modeling (**ORIGEN 2.2**) with atmospheric dispersion analysis (**HotSpot 3.1.2**), it provides a detailed assessment of **TEDE** and **organ-specific CEDE**, particularly highlighting **thyroid vulnerability**. A novel aspect of this research is the use of **localized meteorological data** to simulate real-world seasonal variations in radiological impact zones, thereby offering tailored recommendations for emergency preparedness and radiological protection planning in Bangladesh.

2. MATERIALS AND METHODS

2.1 Overview

This study employs a combined approach using ORIGEN 2.2 and HotSpot 3.1.2 to assess the radiological impact of a hypothetical accident at the Rooppur NPP. The ORIGEN 2.2 code is used to estimate the radionuclide inventory based on operational parameters of the VVER-1200 reactor, including thermal power, fuel enrichment, and burnup data. The calculated source term, representing the types and quantities of radionuclides released during an accident, is then input into the HotSpot code to simulate atmospheric dispersion and dose distribution.

Site-specific meteorological data, such as wind speed, direction, atmospheric stability class, and mixing height, are collected from the Bangladesh Meteorological Department (BMD) and used in the simulation. The general plume model within HotSpot is applied to evaluate airborne dispersion under two seasonal scenarios: rainy and autumn. These conditions reflect varying atmospheric behaviors that can influence the spread and deposition of radioactive materials.

This section outlines the use of dispersion modeling, seasonally variable weather conditions, and validated simulation tools to estimate TEDE and CEDE to the public. The integrated methodology aims to support emergency planning and radiological risk assessment for the Rooppur NPP. The flowchart presented in Figure 1 illustrates the structured methodology adopted in this study to evaluate the health impacts of potential radioactive releases from the Rooppur NPP. The process begins with the identification of the study area, focusing on the Rooppur NPP, which hosts two VVER-1200 pressurized water reactors. Subsequently, reactor core specifications and meteorological data such as wind speed, direction, temperature, and rainfall are collected from the BMD. Radionuclide inventories are calculated using the ORIGEN 2.2 code, while atmospheric dispersion modeling is

conducted with HotSpot 3.1.2. The final phase involves radiation dose estimation and health impact analysis, incorporating both TEDE and organ-specific CEDE, under varying seasonal and spatial conditions.

2.2 Study Area

The study focuses on the Rooppur NPP as shown in Figure 2, located in Ishwardi Upazila of the Pabna District, on the eastern bank of the Padma River in Bangladesh. Geographically, the plant is positioned at approximately 24.068° N latitude and 89.032° E longitude. As Bangladesh's first nuclear power facility, Rooppur NPP consists of two VVER-1200 pressurized water reactors, each with a capacity of 1,200 MWe, developed to address the country's increasing energy demands.

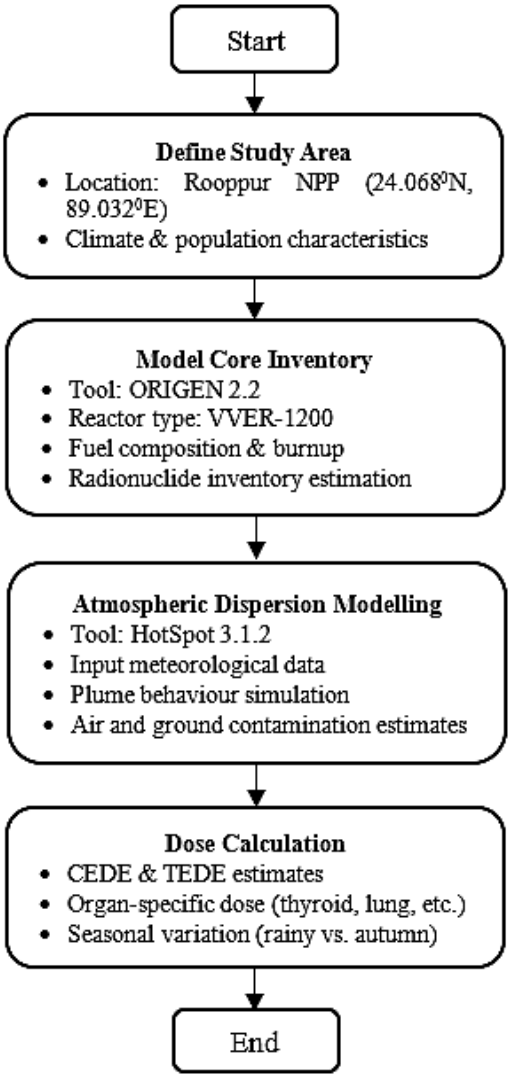

Figure 1: Overview of methodological framework.

Site selection for the plant was guided by detailed feasibility assessments, which considered geological stability, the availability of water resources for reactor cooling, and the relative remoteness from densely populated areas to minimize public risk. The surrounding region is primarily rural, comprising agricultural lands, small settlements, and ecologically sensitive zones, which underscores the critical importance of ensuring public and environmental safety in the event of a radiological incident.

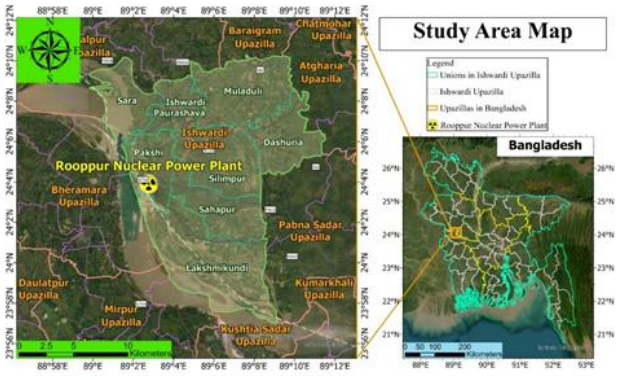

Figure 2: Study area of the Rooppur NPP site.

The area falls under a subtropical monsoon climate, characterized by distinct seasonal variability in meteorological conditions. High precipitation during the rainy season contributes to increased wet deposition of airborne radionuclides, while lower wind speeds in autumn can lead to elevated ground-level concentrations near the release point. These meteorological parameters significantly influence the dispersion behavior of radioactive materials and are therefore central to assessing their potential health impacts.

For this study, site-specific meteorological data, including wind speed, wind direction, temperature, and rainfall, were obtained from the BMD. This data served as input for modeling dispersion and dose assessment using the HotSpot 3.1.2 and ORIGEN 2.2 software tools. The analysis considered a radial distance of up to 40 kilometers from the reactor site, covering zones that may be impacted during a severe nuclear accident.

The selection of this study area allows for a comprehensive assessment of potential radiological health risks to nearby populations and provides a basis for recommending protective measures and emergency response strategies tailored to the specific geographical and climatic conditions of the Rooppur NPP vicinity.

2.3 ORIGEN2.2 Code

ORIGEN2.2 (Croff, 1980; Croff, 1983), developed by Oak Ridge National Laboratory, USA, is a computer code designed to calculate the isotopic composition and associated radiological characteristics of nuclear fuel over time. It models the production and depletion of nuclides due to fission, radioactive decay, neutron capture, and transmutation, making it an essential tool for evaluating source terms in nuclear safety analyses.

The code uses the matrix exponential method to solve a large system of coupled, first-order linear differential equations that describe the time evolution of nuclide concentrations. These equations are based on a point reactor model, assuming a homogeneous system where neutron flux and cross-section values are averaged over space and energy.

The time-dependent concentration of a nuclide X_i is expressed by the following equation (1):

$$\frac{dX_i}{dt} = \sum_{j=1}^{N} l_{ij}\lambda_j X_j + \bar{\Phi}\sum_{k=1}^{N} f_{ik}\sigma_k X_k - X_i(\lambda_i + \bar{\Phi}\sigma_i) \quad (1)$$

Where:

$\bar{\Phi}$: average neutron flux (spatial and energy),
λ_i: decay constant of nuclide i,
σ_i: neutron absorption cross-section of nuclide i,
l_{ij}: fraction of radioactive decay from nuclide j to i,
f_{ik}: fraction of neutron absorption by nuclide k leading to formation of i,
X_i: atomic concentration of nuclide i.

In this study, ORIGEN2.2 was applied to simulate the fission product inventory of the VVER-1200 reactor at Rooppur NPP, using plant-specific data such as core power level, enrichment, burnup, and operational history. The resulting radionuclide inventory serves as the source term input for atmospheric dispersion modeling using the HotSpot code.

2.4 HotSpot Simulation Model

HotSpot 3.1.2 (Homann and Aluzzi, 2013), developed by Lawrence Livermore National Laboratory, is a user-friendly health physics code designed to support emergency planners and first responders in evaluating the radiological consequences of incidents involving radioactive material releases. It employs Gaussian plume atmospheric dispersion models to provide rapid, first-order approximations of radiation impacts due to short-term, short-range, and near-surface radioactive emissions under relatively simple meteorological conditions.

HotSpot is particularly effective in field applications due to its portability, fast computation, and validated performance. Its global recognition and integration into nuclear emergency preparedness tools make it a valuable asset for safety analysis (Malizia et al., 2021). In this study, HotSpot was applied to model a hypothetical radioactive release from the VVER-1200 reactor at Rooppur NPP. The simulation process involved the following key inputs:

- **Source term data** from ORIGEN2.2, which provided the radionuclide inventory and activity,
- **Site-specific meteorological data** such as wind speed, direction, atmospheric stability class, and mixing height (collected from the Bangladesh Meteorological Department),
- **Release conditions**, including release height, duration, and deposition velocity.

Two seasonal scenarios, rainy and autumn, were chosen to reflect different atmospheric dispersion patterns. The primary outputs from the HotSpot simulation included:

- TEDE,
- CEDE due to inhalation of radioactive materials,
- Organ dose for specific human organs exposed to the radiation.

These outputs help determine potential health effects, inform protective actions, and support emergency response planning for hypothetical accident scenarios.

The flowchart of the HotSpot simulation process is illustrated in Figure 3 below.

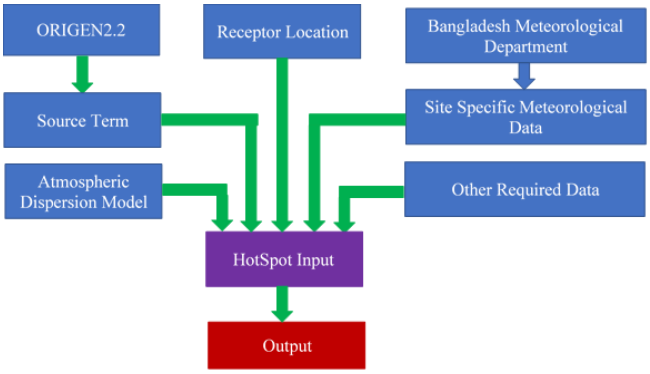

Figure 3: Flowchart illustrating the simulation process of HotSpot (Mawla et al., 2024).

2.5 Meteorological Conditions

Bangladesh has six traditional seasons; however, for the purpose of this study, four primary seasons have been considered due to their meteorological significance: winter (December–February), summer (March–May), rainy season (June–September), and autumn (October–November) (Ayesha et al., 2016). The country experiences a tropical monsoon climate, marked by notable variations in temperature, humidity, and rainfall across these seasons.

During the summer, long sunny days and high temperatures dominate. The rainy season is characterized by heavy cloud cover and frequent, intense rainfall. The autumn season generally features lower rainfall and slightly cooler temperatures, while winter brings the lowest temperatures of the year.

Meteorological conditions at the Rooppur NPP site are particularly important for both routine operations and emergency preparedness. Wind speed, direction, temperature gradients, and atmospheric stability significantly influence the dispersion of radioactive materials in the event of an accidental release. This study specifically focuses on two representative seasons, rainy and autumn, to evaluate atmospheric dispersion behavior and radiological impacts under varying weather conditions.

2.5.1 Rainy Season

The rainy season, also known as the southwest monsoon, spans June through September and is characterized by persistent cloud cover, frequent rainfall, and high humidity (Ayesha et al., 2016). During this period, wind predominantly flows from the east, with occasional movement from the south.

The wind rose analysis of the last thirty-two years, presented in Figure 4, illustrates the seasonal wind direction and frequency patterns for the Rooppur region. Based on this long-term data, the average wind speed during the rainy season is 1.64 m/s, while the calm wind frequency stands at 30.7%. Wind speeds ranging from 0.50–2.10 m/s occur 27.3% of the time, 2.10–3.60 m/s occur 22.5%, and 3.60–5.70 m/s occur 7.9%.

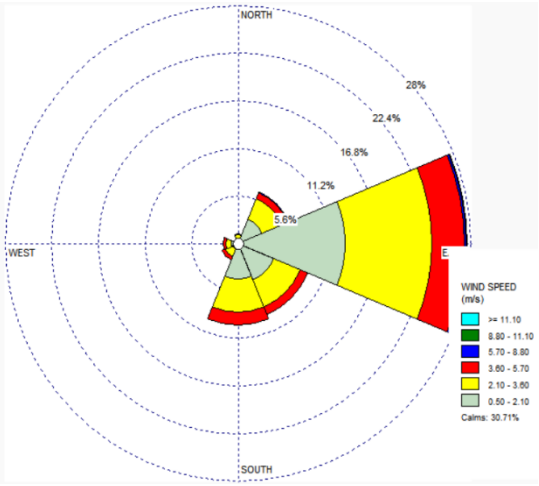

Figure 4: The wind rose for the average wind speed of the rainy season.

Relative humidity is generally high throughout the season, often exceeding 80%, which can significantly affect atmospheric dispersion. According to the BMD, the average rainfall during this period is approximately 0.65 mm/hr. Wind conditions are typically light to moderate (Ayesha et al., 2016), influencing the surface-level concentration and movement of airborne radioactive materials in the event of a nuclear release.

2.5.2 Autumn Season

The autumn season, also referred to as the post-monsoon period, encompasses the months of October and November (Ayesha et al., 2016). During this season, the prevailing wind direction is primarily from the east, with occasional flows from the northeast and west.

The wind rose analysis over the past thirty-two years, shown in Figure 5, illustrates the seasonal wind patterns specific to this period. The average wind speed during autumn is 0.95 m/s, the lowest among all four seasons, indicating reduced atmospheric dispersion capacity. The calm wind frequency is notably high at 53.2%. Wind speeds between 0.50–2.10 m/s occur 19.5% of the time, 2.10–3.60 m/s occur 12.5%, and 3.60–5.70 m/s occur only 3.4%.

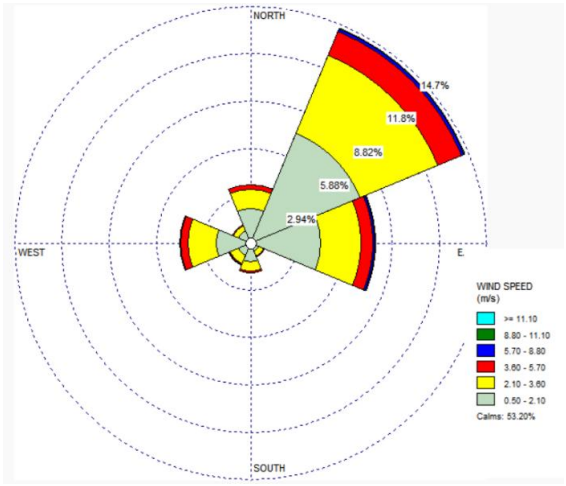

Figure 5: The wind rose for the average wind speed of the autumn season

Meteorological data from the BMD show that the average rainfall during autumn is 0.15 mm/hr, indicating relatively dry conditions compared to the rainy season. Additionally, the month of November records the lowest average wind speed of 0.89 m/s and the highest calm wind frequency of 55.21%.

2.5.3 Atmospheric Stability

Atmospheric stability refers to the behavior of an air parcel when it is slightly displaced vertically, determining whether it will rise, sink, or remain in equilibrium. This property is crucial in assessing how radioactive materials released during a nuclear incident disperse in the atmosphere. Factors such as temperature gradients, wind speed, and wind direction significantly influence atmospheric stability and, consequently, the dispersion patterns of radioactive plumes (Hussain et al., 2023). Accurate characterization of atmospheric stability is essential for predicting the spread and concentration of radionuclides, which directly impacts the radiological risk to the environment and public health. The Pasquill stability classification is commonly used to categorize atmospheric conditions into six classes: A (very unstable), B (moderately unstable), C (slightly unstable), D (neutral), E (slightly stable), and F (moderately stable) (Foudil et al., 2017; Ned Xoubi, 2020). These classifications are critical inputs for dispersion models like HotSpot, which use them to simulate the transport and deposition of radioactive substances under various meteorological scenarios.

3. RESULTS AND DISCUSSIONS

3.1 Overview

In this study, the worst-case scenario is modeled based on current meteorological data, where Stability Class A, representing very unstable atmospheric conditions, is assumed to produce the highest radiological impact. For the sake of conservative assessment, the effective release height is considered to be zero meters, simulating a containment failure with ground-level discharge. Several human organs are susceptible to radiation exposure during a severe nuclear accident; however, this analysis focuses on the thyroid, skin, lungs, surface bone, red bone marrow, and liver due to their radiosensitivity and relevance to dose assessment. To simplify calculations in the HotSpot code, an effective population of 50 individuals is assumed within the exposure zone. Distances from the source are defined arbitrarily within the model to evaluate plume dispersion and resulting organ doses.

3.2 Calculation of the Source Term

The core inventory of radionuclides was assessed using the ORIGEN 2.2 code, which calculates the time-dependent activity of each nuclide based on fuel composition, burnup history, and operational parameters. To estimate the source term released during a hypothetical accident, group-specific release fractions were applied to the core inventory. The radionuclides were categorized into chemical groups, namely noble gases, halogens, alkali metals, tellurium, and lanthanides. The distribution of radionuclides by group is presented in Table 1, while Table 2 lists the individual radionuclides along with their

corresponding activity values in Becquerels (Bq).

Table 1: Formation of source term with different groups

Nuclide Group	Species	Total Activity (Bq)	Percentage (%)
Noble Gas	Kr, Xe	1.81×10^{19}	62.60
Halogen	I	7.81×10^{18}	26.94
Alkali metal	Ba, Cs	2.34×10^{18}	8.06
Tellurium	Te	6.93×10^{17}	2.39
Lanthanide	Y	3.22×10^{15}	0.01

Among the groups, noble gases and halogens represent the most significant contributors to the total inventory, with activities of approximately 1.81×10^{19} Bq and 7.81×10^{18} Bq, respectively. These high activity levels are attributed to their volatility and low retention in containment systems. Figure 6 visualizes the activity levels of each radionuclide group in the reactor core following a postulated accident scenario at the Rooppur NPP, highlighting the dominant role of noble gases and halogens in defining the source term.

To evaluate the environmental impact and associated health risks of various radionuclide groups, ground-level deposition was computed independently for each chemical category. Radioisotopes were selected as representative source terms, grouped into three primary classes. Table 2 provides a detailed overview of each isotope's core inventory, applied release fraction, and corresponding released activity. These findings were benchmarked against international data from multiple nuclear reactors, demonstrating consistency with previous studies conducted by the IAEA (2008), Anvari (2012) and Foudil et al. (2017). The observed variations across datasets are attributed to differences in reactor types, fuel compositions, burnup levels, and radionuclide inventories (Ned Xoubi, 2022).

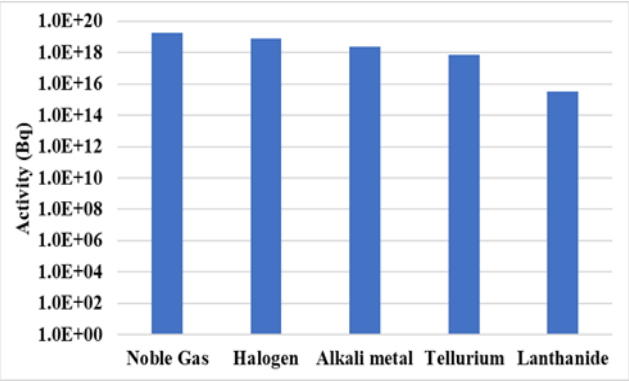

Figure 6: Groupwise core inventory.

Each radionuclide poses distinct health hazards depending on its radiological properties and biological uptake mechanisms. For example, the core inventory of Iodine-131 (^{131}I) was estimated at 2.97×10^{18} Bq, with 1.19×10^{18} Bq released into the environment. In comparison, Cesium-137 (^{137}Cs) had a core inventory of 3.27×10^{17} Bq, of which 9.81×10^{16} Bq was released. These estimates are based on a hypothetical worst-case scenario involving complete core exposure and a full containment breach at the Rooppur NPP.

Table 2: Source Term of VVER-1200 Reactor Core

Nuclide	Core Inventory (Bq)	Release Fraction (NRC 1.183)	Release to Environment (Bq)
^{83m}Kr	4.11×10^{17}	1	4.11×10^{17}
^{85}Kr	3.19×10^{16}	1	3.19×10^{16}
^{85m}Kr	8.99×10^{17}	1	8.99×10^{17}
^{87}Kr	1.75×10^{18}	1	1.75×10^{18}
^{88}Kr	2.47×10^{18}	1	2.47×10^{18}
^{89}Kr	3.06×10^{18}	1	3.06×10^{18}
^{133}Xe	6.23×10^{18}	1	6.23×10^{18}
^{133m}Xe	1.92×10^{17}	1	1.92×10^{17}
^{128}I	2.81×10^{16}	0.4	1.12×10^{16}
^{130}I	8.79×10^{16}	0.4	3.52×10^{16}
^{131}I	2.97×10^{18}	0.4	1.19×10^{18}
^{132}I	4.32×10^{18}	0.4	1.73×10^{18}
^{133}I	6.25×10^{18}	0.4	2.50×10^{18}
^{135}I	5.85×10^{18}	0.4	2.34×10^{18}
^{139}Ba	5.69×10^{18}	0.02	1.14×10^{17}
^{140}Ba	5.48×10^{18}	0.02	1.09×10^{17}
^{134}Cs	4.87×10^{17}	0.3	1.46×10^{17}
^{134m}Cs	1.30×10^{17}	0.3	3.90×10^{16}
^{135m}Cs	7.66×10^{16}	0.3	2.30×10^{16}
^{136}Cs	1.53×10^{17}	0.3	4.59×10^{16}
^{137}Cs	3.27×10^{17}	0.3	9.81×10^{16}
^{138}Cs	5.85×10^{18}	0.3	1.76×10^{18}
^{90}Y	2.63×10^{17}	0.0002	5.26×10^{13}
^{91}Y	4.23×10^{18}	0.0002	8.26×10^{14}
^{91m}Y	2.38×10^{18}	0.0002	4.76×10^{14}
^{92}Y	4.38×10^{18}	0.0002	8.76×10^{14}
^{93}Y	4.96×10^{18}	0.0002	9.92×10^{14}
^{127}Te	2.83×10^{17}	0.05	1.42×10^{16}
^{127m}Te	3.75×10^{16}	0.05	1.88×10^{15}
^{129}Te	8.91×10^{17}	0.05	4.46×10^{16}
^{129m}Te	1.33×10^{17}	0.05	6.65×10^{15}
^{131m}Te	4.19×10^{17}	0.05	2.10×10^{16}
^{132}Te	4.26×10^{18}	0.05	2.13×10^{17}
^{133m}Te	2.39×10^{18}	0.05	1.19×10^{17}
^{134}Te	5.43×10^{18}	0.05	2.72×10^{17}

To ensure a conservative and safety-focused approach, standard release fractions were applied based on established guidelines and previous literature, including NRC Regulatory Guide 1.183 (2000). Under these assumptions, the total source term released into the environment from the Rooppur NPP, as modeled using the HotSpot code, is estimated at 2.90×10^{19} Bq. Among the selected radionuclides, Iodine-131 (^{131}I) and Cesium-137 (^{137}Cs) emerged as key contributors due to their high radioactivity and environmental persistence, which make them significant threats through contamination of air, water, soil, and food chains. Additionally, Iodine-133 (^{133}I) showed the highest individual release at 2.50×10^{18} Bq, followed by Xenon-133 (^{133}Xe) at 6.23×10^{18} Bq highlighting the critical roles of halogens and noble gases in the overall radiological impact. These results closely align with global data from similar reactor studies, accounting for differences in fuel design and operating conditions. Subsequent sections further examine the

HotSpot simulation outputs under the prevailing meteorological conditions to assess the potential dose impacts on human organs and the surrounding environment.

3.3 Description of TEDE

3.3.1 TEDE in rainy season

During the rainy season, the highest recorded TEDE along the plume center line was 3.80 × 10^4 Sv, observed within 30 meters of the reactor core. This value decreased rapidly by two orders of magnitude within six minutes, reaching 9.40 × 10^2 Sv at 300 meters from the source. The dose continued to drop by another order of magnitude, measuring 2.20 × 10^1 Sv at 3 kilometers after approximately one hour and two minutes. The declining trend persisted over time and distance, reducing to 1.60 × 10^{-5} Sv at 30 kilometers after ten hours and twenty-eight minutes. At a distance of 70 kilometers, the TEDE further declined to 1.30 × 10^{-13} Sv, occurring more than twenty-four hours post-release. The variation of dose and activity with distance for both the rainy and autumn seasons is illustrated in Figure 7.

3.3.2 TEDE in Autumn Season

During the autumn season, the peak TEDE at the plume centerline was recorded as 5.5 × 10^4 Sv at a distance of 30 meters from the reactor core, occurring within less than one minute of the release. This value decreased by two orders of magnitude to 7.8 × 10^2 Sv at 300 meters from the source within approximately five minutes. The dose continued to diminish, reaching 2.1 × 10^1 Sv at 3 kilometers after fifty-eight minutes. At a distance of 30 kilometers, the TEDE further dropped to 1.4 × 10^{-2} Sv after nine hours and forty-nine minutes. Eventually, at 70 kilometers, the dose declined to 4.5 × 10^{-6} Sv within twenty-two hours and fifty-four minutes. The variation of dose with distance across different seasons is illustrated in Figure 7.

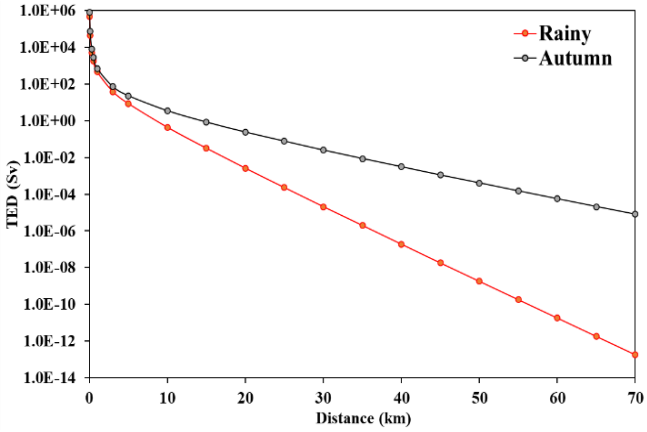

Figure 7: TEDE Vs Distance in rainy and autumn seasons.

3.3.3 Comparison of TEDE

The maximum TEDE values for the rainy and autumn seasons were observed at a distance of 0.030 km (30 meters) from the reactor site, registering 3.8 × 10^4 Sv and 5.5 × 10^4 Sv, respectively (Figure 7). This variation is primarily attributed to differences in wind speed between the two seasons: the autumn season experiences the lowest average wind speed at 0.95 m/s, while the rainy season records the highest at 1.64 m/s. From the source, TEDE values exhibit a steep decline within the first 300 meters, after which the decrease becomes more gradual over time and distance. These findings are consistent with those of Hussain et al., (2023), which similarly concluded that higher wind speeds contribute to lower peak TEDE values due to enhanced dispersion. Importantly, the doses measured during the first hour of exposure significantly exceed public dose limits established by regulatory authorities.

3.4 Individual Organ Dose

The impact of radiation on human health and the environment was assessed using site-specific meteorological data and radionuclide profiles relevant for plume dose estimation. The HotSpot code was employed to calculate the CEDE, which integrates committed dose equivalents over a 50-year period for various body organs, weighted by appropriate tissue weighting factors (Henry et al., 2021). In the event of a severe nuclear accident, radiation exposure can affect human organs, including the skin, lungs, thyroid, surface bone, red marrow, liver, spleen, adrenal glands, ovaries, breasts, stomach wall, small intestine wall, upper and lower large intestine walls, bladder wall, thymus, esophagus, muscle, kidneys, testes, uterus, pancreas, and brain. However, the subsequent discussion focuses on the most radiosensitive organs and compares their responses under different seasonal conditions.

3.4.1 Individual Organ Dose in Rainy Season

Figure 8 presents the CEDE distribution across critical organs, including the thyroid, skin, lungs, surface bone, red marrow, and liver, as a function of downwind distance during the rainy season. Among these, the thyroid exhibits the highest sensitivity, receiving the most significant dose of CEDE. The maximum dose for the thyroid is estimated at 4.7×10^5 Sv at a distance of 0.03 km from the reactor, occurring within the first minute of release.

Following the thyroid, the organs with the highest CEDE values at 30 meters include the skin (5.7×10^4 Sv), lungs (1.5×10^4 Sv), surface bone (2.1×10^4 Sv), red marrow (1.4 × 10^4 Sv), and liver (1.3×10^4 Sv). These doses decline sharply with increasing distance and time. At 300 meters, within approximately three minutes, the CEDE values reduce to 5.0×10^3 Sv (thyroid), 3.1 × 10^3 Sv (skin), 7.0×10^2 Sv (lungs), 1.0×10^3 Sv (surface bone), 7.1 × 10^2 Sv (red marrow), and 6.6 × 10^2 Sv (liver).

The trend of dose reduction continues at greater distances. At 3 km, within thirty-four minutes post-release, the thyroid receives 3.9×10^1 Sv, followed by the skin (9.2 × 10^1 Sv), lungs (2.0×10^1 Sv), surface bone (2.9 × 10^1 Sv), red marrow (2.1×10^1 Sv), and liver (1.9×10^1 Sv). At 20 km, after three hours and forty-seven minutes, the CEDE values further decline to 2.6 × 10^{-3} Sv (thyroid), 8.7 × 10^{-3} Sv (skin), 1.8×10^{-3} Sv (lungs), 2.7×10^{-3} Sv (surface bone), 1.9×10^{-3} Sv (red marrow), and 1.7×10^{-3} Sv (liver). These observations highlight the rapid attenuation of organ doses

with increasing distance and time after the release.

3.4.2 Individual organ dose in the autumn season

Figure 9 illustrates the distribution of CEDE across key human organs, specifically the thyroid, skin, lung, surface bone, red marrow, and liver, as a function of downwind distance during the autumn season. Among these, the thyroid is identified as particularly sensitive, receiving the highest CEDE values shortly after release. The maximum CEDE for the thyroid was observed at 0.030 km from the release point, estimated at 8.0×10^5 Sv within the first minute. Other organs also exhibited elevated doses at this distance: the skin (5.4×10^4 Sv), lung (1.6×10^4 Sv), surface bone (2.2×10^4 Sv), red marrow (1.5×10^4 Sv), and liver (1.4×10^4 Sv).

Doses decrease significantly with increasing distance and time. At 300 meters, within approximately three minutes of release, CEDE values dropped to: thyroid (8.0×10^3 Sv), skin (1.6×10^3 Sv), lung (3.9×10^2 Sv), surface bone (5.6×10^2 Sv), red marrow (3.9×10^2 Sv), and liver (3.6×10^2 Sv).

By the time the plume reached 3 km, roughly fifty-eight minutes post-release, organ doses further declined: thyroid (7.2×10^1 Sv), skin (7.9×10^1 Sv), lung (1.7×10^1 Sv), surface bone (2.5×10^1 Sv), red marrow (1.8×10^1 Sv), and liver (1.6×10^1 Sv).

At 35 km, nearly eleven and a half hours after the release, the CEDE levels were significantly reduced but still measurable: thyroid (8.7×10^{-3} Sv), skin (2.3×10^{-2} Sv), lung (4.6×10^{-3} Sv), surface bone (6.9×10^{-3} Sv), red marrow (4.7×10^{-3} Sv), and liver (4.4×10^{-3} Sv).

3.4.3 Analysis on Individual Organ Dose

The CEDE is highest near the reactor in both seasons and decreases with time and distance due to plume dispersion and dilution. Lower wind speeds result in higher CEDE values; thus, the autumn season, with an average wind speed of 0.95 m/s, shows greater doses than the rainy season (1.64 m/s), as illustrated in Figures 8 and 9.

At 0.030 km, CEDE values peak for all organs, especially the thyroid (8.0×10^5 Sv in autumn). Other affected organs in descending order are skin (5.4×10^4 Sv), surface bone (2.2×10^4 Sv), lung (1.6×10^4 Sv), red marrow (1.5×10^4 Sv), and liver (1.4×10^4 Sv). These six organs are the most vulnerable to radiation in severe accident scenarios at Rooppur NPP.

In the rainy season, CEDE declines more sharply beyond 10 km, becoming negligible by 20 km due to atmospheric washout from rainfall (0.65 mm/hr). In contrast, the autumn season maintains significant CEDE levels up to 30 km due to minimal precipitation.

Exposures above 0.1 Sv increase cancer risk by 0.5%, per ICRP guidelines (ICRP, 2007). In autumn, CEDE exceeds this threshold up to 20 km, posing health risks to the public. Occupational exposure limits set by the USNRC (50 mSv/year) are exceeded up to 17 km in the rainy season and 30 km in autumn, indicating extended risk zones for workers.

To mitigate internal exposure from inhaled or ingested radionuclides, emergency measures such as evacuation, sheltering, and stable iodine prophylaxis are essential, especially for protecting sensitive organs like the thyroid (Henry et al., 2021).

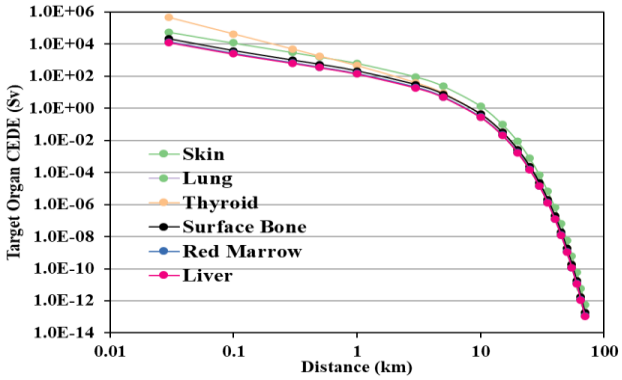

Figure 8: Organ CEDE versus downwind distance in the rainy season.

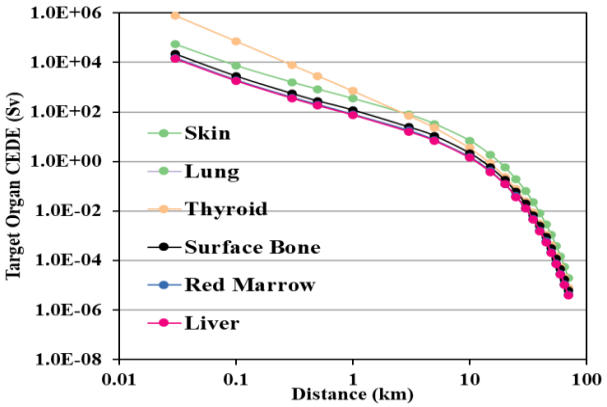

Figure 9: Organ CEDE versus downwind distance in the autumn season.

3.5 Thyroid Committed Dose Equivalent

Radioactive iodine released during a nuclear power plant accident poses a significant health risk, particularly to the thyroid gland. Due to its natural affinity for iodine, the thyroid readily absorbs radioactive isotopes, making it highly susceptible to radiation damage. This can result in both immediate and long-term health effects, including an increased risk of thyroid disorders and cancer.

3.5.1 Thyroid CEDE in Rainy Season.

According to NNREPRP guidelines, the permissible thyroid dose is 50 mSv within the first 7 days following a nuclear incident (NNREPRP, 2020). During the rainy season, thyroid CEDE levels vary significantly with distance from the reactor, as illustrated in Figure 10. The highest doses are observed near the reactor site, gradually decreasing with increasing distance and time. For atmospheric stability class A, individuals within a 15 km radius are likely to receive thyroid doses exceeding the regulatory limit. Beyond this distance, radiation exposure drops to negligible levels. Consequently, emergency protective actions, including relocation to nearby shelters, are strongly recommended for populations residing within the 15 km zone.

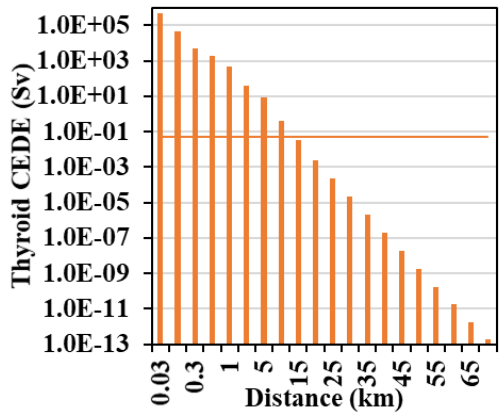

Figure 10: Comparison of radiation doses for the thyroid with the generic criteria of IAEA in the rainy season

3.5.2 Thyroid CEDE in Autumn Season

As specified by the NNREPRP, the permissible thyroid dose is 50 mSv over the first 7 days following a radiological incident (NNREPRP, 2020). In the autumn season, the distribution of thyroid CEDE varies notably with distance from the reactor site, as illustrated in Figure 11. Radiation exposure is highest in close proximity to the reactor and gradually declines with both time and increasing distance. Under stability class A conditions, individuals within a 27.5 km radius are likely to receive thyroid doses exceeding the allowable limit. Beyond this range, the exposure is considered minimal. Consequently, populations within the 27.5 km zone should be promptly relocated to appropriate shelters as part of emergency protective measures.

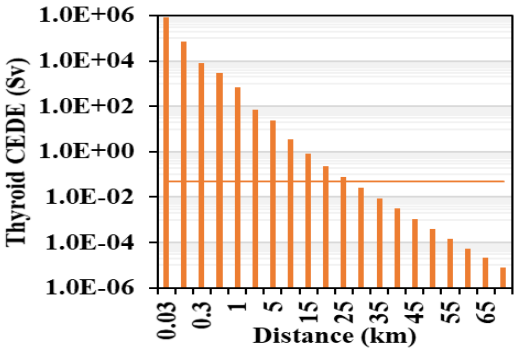

Figure 11: Comparison of radiation doses for thyroid with generic criteria of IAEA in the autumn season

3.5.3 Analysis of Thyroid CEDE

The highest thyroid CEDE values recorded were 4.48 × 10^5 Sv during the rainy season and 7.18 × 10^5 Sv during the autumn season at a distance of 30 meters from the source (Figures 9 and 10). Although radiation exposure declines with distance, elevated doses remain a concern. CEDE values exceeded the safety threshold of 50 mSv up to 15 km in the rainy season and 27.5 km in the autumn season. Beyond these distances, the measured thyroid doses dropped to levels considered negligible, largely due to the dispersive effects of wind and precipitation.

In situations where thyroid dose limits are surpassed, the administration of stable iodine, specifically potassium iodide (KI), is essential as a protective countermeasure. KI effectively saturates the thyroid with non-radioactive iodine, thereby reducing the uptake of radioactive iodine isotopes. The U.S. Food and Drug Administration (FDA) bases KI dosing guidelines (NRC000075, 2001) on findings from the Chernobyl nuclear accident, emphasizing early administration, especially for children and pregnant women. The most conservative intervention level is an internal thyroid exposure exceeding 0.05 Sv (50 mSv), which warrants the use of KI for all age groups, as shown in Table 3.

Table 3: Recommended doses of KI for the thyroid gland (NRC000075, 2001)

Thyroid dose (mSv)	KI concentration dose (mg)	Risk group age
≥5000	130	Over 40 yr
≥10000	130	Over 18 to 40 yr
≥50	130 16–65 (with consideration of different weight)	Pregnant women Infants within 1 month to adolescents with 18 yr

4. CONCLUSIONS

This study provided a detailed evaluation of radiological dose consequences, specifically TEDE and CEDE, for individual human organs in the event of a severe nuclear accident scenario at the Rooppur NPP. The analysis was carried out for different atmospheric stability conditions across two representative seasons: the rainy and autumn periods. Using atmospheric dispersion modeling and dose estimation tools, the study assessed radiation exposure as a function of distance, time, and meteorological variability.

In terms of TEDE, which incorporates both external and internal exposure pathways, the results showed similarly elevated dose values near the release point. TEDE assessments reinforce that radiation doses within the first 15 km (rainy season) and 27.5 km (autumn season) surpass the allowable exposure limits for the general public and even exceed occupational safety thresholds in certain cases. For instance:

- The ICRP recommended dose limit of 100 mSv (ICRP, 2007) for cancer risk becomes relevant within 20 km in autumn.
- The USNRC annual occupational TEDE limit of 50 mSv is exceeded up to 17 km in the rainy season and 30 km in the autumn season.

The results indicate that the thyroid gland is the most critically exposed organ, with maximum CEDE values reaching 8.0 × 10^5 Sv at 0.03 km during the autumn season. The elevated exposure is attributed to the thyroid's high biological affinity for radioactive iodine and the season's low wind speed (0.95 m/s), which limits plume dispersion. In comparison, the rainy season showed lower thyroid CEDE values (4.7 × 10^5 Sv at 0.03 km), influenced by higher wind speed (1.64 m/s) and rainfall (0.65 mm/hr), which contributed to faster dilution and deposition of radioactive particles.

CEDE to other organs such as the skin, lung, surface bone, red marrow, and liver also showed elevated levels in close

proximity to the reactor, with doses decreasing significantly over time and distance. These organs demonstrated radiation sensitivity, with implications for both deterministic and stochastic health effects. Maximum CEDE values at 30 meters exceeded internationally recommended dose thresholds, warranting urgent protective measures.

These findings emphasize the necessity of both CEDE and TEDE metrics in comprehensive radiological risk evaluation and emergency planning.

To mitigate thyroid exposure specifically, the use of KI as a thyroid-blocking agent is strongly recommended when thyroid CEDE exceeds 50 mSv. Based on FDA guidance, KI administration should be prioritized for vulnerable groups such as infants, children, adolescents, and pregnant women. Dose-specific intervention levels must be tailored based on estimated thyroid CEDE, as outlined in KI dosage guidelines (Table 3 of this study).

Based on these findings, the following conclusions and recommendations are proposed:

- emergency planning zones (EPZs) must be established, considering variations in CEDE and TEDE distributions.
- Evacuation, sheltering, and stable iodine administration should be promptly implemented within 15–30 km of the reactor depending on the season and real-time atmospheric conditions.
- First responders and reactor personnel must be equipped with appropriate protective gear and dosimetry, given the exceedance of occupational TEDE limits in key zones.
- Integration of CEDE and TEDE modeling into national nuclear emergency preparedness frameworks like NNREPRP is essential for realistic response planning.
- Continuous training, simulation, and meteorological monitoring must be maintained to enhance response effectiveness under variable scenarios.

In conclusion, this study highlights that both CEDE and TEDE are critical indicators of radiation risk following a nuclear accident. A multi-organ and multi-seasonal dose evaluation approach is vital for informed decision-making. The results strongly support the enhancement of public health protection protocols and emergency preparedness plans for Rooppur NPP and other nuclear facilities in similar settings.

DATA AVAILABILITY STATEMENT

Datasets generated during the current study are available from the corresponding author upon reasonable request.

FUNDING DECLARATION

This research was self-funded.

ETHICS APPROVAL

This study is an engineering experimental investigation. The MIJST Research Ethics Committee has confirmed that formal ethical approval was not required.

ETHICS, CONSENT TO PARTICIPATE, AND CONSENT TO PUBLISH

Not applicable.

COMPETING INTERESTS

The authors declare that they have no competing interests.

AUTHOR CONTRIBUTIONS

Author 1: Md Rosaidul Mawla1 – Methodology, Investigation, Writing manuscript

Author 2: Radmim Ryean – Investigation, Data curation

Author 3: Anisur Rahman - Validation, manuscript revision

Author 4: Abdus Sattar Mollah - Resources, manuscript revision

Author 5: Md. Shafiqul Islam - Visualization, manuscript revision

Author 6: Kazi Imtiaz Kabir – Visualization, manuscript revision

ARTIFICIAL INTELLIGENCE ASSISTANCE STATEMENT

Portions of this manuscript were assisted by an artificial intelligence language model (ChatGPT, OpenAI). The tool was used solely for language editing, text refinement, and clarity improvement. All content, data interpretation, analysis, conclusions, and final decisions were generated, verified, and approved by the authors. The authors take full responsibility for the accuracy and integrity of the manuscript.

CONFLICT OF INTEREST DECLARATION

The authors declare that they have no conflicts of interest.

REFERENCES

Aliyu, A. S., Ramli, A. T., Saleh, M. A. (2015). Assessment of potential human health and environmental impacts of a nuclear power plant (NPP) based on atmospheric dispersion modeling, Atmósfera 28(1), 13-26, https://doi.org/10.1016/S0187-6236(15)72156-9

Anvari, A., Safarzadeh, L. (2012). Assessment of the total effective dose equivalent for accidental release from the Tehran Research Reactor, Annals of Nuclear Energy, 50, 251-255. https://doi.org/10.1016/j.anucene.2012.07.002

Ayesha, M. K., Rashid, M. B., Hygen, H. O. (2016). MET report on Climate of Bangladesh no. 08/2016, ISSN 2387-4201, https://live6.bmd.gov.bd/file/2016/08/17/pdf/21827.pdf

Croff, A. G., & Oak Ridge National Lab., TN (USA). (1980). User's manual for the ORIGEN2 computer code, ORNL/TM-7175.

Croff, A. G. (1983). ORIGEN2: A versatile computer code for calculating the nuclide compositions and

characteristics of nuclear materials. Nucl. Technol., 62(3), 335–352.

Fairuz, A., Sahadath M. H. (2020). Characterization of Atmospheric Radiological Dispersion alongside Risky Location Designation and Shelter House Proposition around the Planned Rooppur Nuclear Power Plant (RNPP)", Journal of Nuclear Engineering and Radiation Science, 6(4), 042003, https://doi.org/10.1115/1.4046670

Faith, R., Kim, J. (2020). Assessment of Lifetime Attributable Risk for Public Health Sustainability from the Fukushima Accident, Science and Technology of Nuclear Installations, 2020(2020), 1-6, 8873031, https://doi.org/10.1155/2020/8873031

Foudil, Z., Mohamed, B., Tahar, Z. (2017). Estimating of core inventory, source term and doses results for the NUR research reactor under a hypothetical severe accident, Progress in Nuclear Energy, 100, 365–372. https://doi.org/10.1016/j.pnucene.2017.07.013

Henry, K. O., Sylvester, A. B., Gyamfi, K., Simon, A., Andrew, N. (2021), Assessment of radiological consequence of a hypothetical accident at the Ghana Research Reactor-1 facility based on terrorist attack. Science Progress, 104(4), 1-24. doi:10.1177/00368504211054986

Hoeve J. E. T., Jacobson M. Z. (2012). Worldwide health effects of the Fukushima Daiichi nuclear accident. Energ. Environ. Sci. 5(9), 8743-8757, https://doi.org/10.1039/C2EE22019A

Homann, S. G., Aluzzi, F. (2013). HOTSPOT Health Physics Codes Version 3.0 User's Guide, National Atmospheric Release Advisory Center, Lawrence Livermore National Laboratory, LLNL-SM-636474.

Hussain, M., Mehboob, K., Ilyas S. Z., Shaheen S. (2023). Implications of Local Scale Meteorological Data on Radioactive Plume Dispersion and Dose Delivery for a Hypothetical Severe Accident at PARR-1. Arab J Sci Eng 48, 739–755. https://doi.org/10.1007/s13369-022-06998-w

IAEA, (2008). Derivation of the source term and analysis of the radiological consequences of research reactor accidents. Safety reports series No. 53, International Atomic Energy Agency, Vienna, Austria.

IAEA, (2013). Actions to Protect the Public in an Emergency due to Severe Conditions at a Light Water Reactor, Emergency preparedness and response, EPR-NPP-PPA, International Atomic Energy Agency, Vienna, Austria.

ICRP, (2007). ICRP Publication 103: The 2007 Recommendations of the International Commission on Radiological Protection, Ann. ICRP, 37(2.4), p. 2.

ICRU, 2015. Major releases of radionuclides to the environment, Journal of the International Commission on Radiation Units and Measurements, 15(1-2), 4–36, https://doi.org/10.1093/jicru_ndy01

Malizia, A., Chierici, A., Sergio, B., Marco, D., Ludovici, G. M., Francesco, d., Guglielmo, M., Fabio M. (2021). The HotSpot Code as a Tool to Improve Risk Analysis During Emergencies: Predicting I-131 and CS-137 Dispersion in the Fukushima Nuclear Accident, International Journal of Safety and Security Engineering, 11(4), 473-486, https://doi.org/10.18280/ijsse.110421

Mawla, M. R., Rahman, A., Mollah, A. S., Ryean, R., Islam, M. S. (2024). Assessment of radiological consequences to a hypothetical accident of the 3-MW TRIGA Mark-II nuclear research reactor of Bangladesh, Nuclear Engineering and Design, 424, https://doi.org/10.1016/j.nucengdes.2024.113255

Mollah, A. S., Sattar, S., Hossain, A., Salahuddin, M., Khan, A. Z., Hossain, M. S. (2016). Review and analysis of environmental impacts of different energy technologies: clean environment from nuclear energy, MIST Journal of Science and Technology, Vol. 4(1), 1-13, ISSN 2224-2007

Ned Xoubi. (2020). Assessment of environmental radioactive surface contamination from a hypothetical nuclear research reactor accident. Heliyon, 6(9), 1-8, https://doi.org/10.1016/j.heliyon.2020.e04968

NNREPRP (2020). National Nuclear and Radiological Emergency Preparedness and Response Plan (NNREPRP). Ministry of Science and Technology, Government of the People's Republic of Bangladesh.

NRC000075, (2001). Potassium Iodide as a Thyroid Blocking Agent in Radiation Emergencies, U.S. Department of Health and Human Services, Food and Drug Administration, Center for Drug Evaluation and Research (CDER).

NRC 1.183, (2000). Alternative Radiological Source Terms for Evaluating Design Basis Accidents at Nuclear Power Reactors, U.S. Nuclear Regulatory Commission Regulatory Guide.

Rogner, H.-H. (2001). Nuclear Power and Sustainable Energy Development. The Journal of Energy and Development, 26(2), 235–258. http://www.jstor.org/stable/24808916

Sihver, L., Yasuda, N. (2018). Causes and Radiological Consequences of the Chernobyl and Fukushima Nuclear Accidents, Journal of Nuclear Engineering and Radiation Science, NERS-16-1166, 4(2), 020914, https://doi.org/10.1115/1.4037116

Walsh, L., Zhang, W., Shore, R. E., Auvinen, A., Laurier, D., Wakeford, R., Jacob, P., Gent, N., Anspaugh, L. R., Schüz, J., Kesminiene, A., van Deventer, E., Tritscher, A., del Rosarion Pérez, M. (2014). A framework for estimating radiation-related cancer risks in Japan from the 2011 Fukushima nuclear accident, Radiation Research, 182(5), 556-572, https://doi.org/10.1667/RR13779.1

Yasunari, T. J., Stohl, A., Hayano, R. S., Burkhart, J. Eckhardt, F., S., Yasunari, T. (2011). Cesium-137 deposition and contamination of Japanese soils due to the Fukushima nuclear accident. P. Natl. Acad. Sci. USA, 108(49), 19530-19534, https://doi.org/10.1073/pnas.1112058108